J Electr Eng Technol.2017; 12(4): 1442-1448
http://doi.org/10.5370/JEET.2017.12.4.1442

ISSN(Print) 1975-0102
ISSN(Online) 2093-7423

# Application of Superconducting Flywheel Energy Storage System to Inertia-Free Stand-Alone Microgrid

**SunHo Bae*, DongHee Choi*, Jung-Wook Park* and Soo Hyoung Lee†**

**Abstract** – Recently, electric power systems have been operating with tight margins and have reached their operational limits. Many researchers consider a microgrid as one of the best solutions to relieve that problem. The microgrid is generally powered by renewable energies that are connected through power converters. In contrast to the rotational machines in the conventional power plants, the converters do not have physical rotors, and therefore they do not have rotational inertia. Consequently, a stand-alone microgrid has no inertia when it is powered by the only converter-based-generators (CBGs). As a result, the relationship between power and frequency is not valid, and the grid frequency cannot represent the power balance between the generator and load. In this paper, a superconducting flywheel energy storage system (SFESS) is applied to an inertia-free stand-alone (IFSA) microgrid. The SFESS accelerates or decelerates its rotational speed by storing or releasing power, respectively, based on its rotational inertia. Then, power in the IFSA microgrid can be balanced by measuring the rotor speed in the SFESS. This method does not have an error accumulation problem, which must be considered for the state of charge (SOC) estimation in the battery energy storage system (BESS). The performance of the proposed method is verified by an electromagnetic transient (EMT) simulation.

**Keywords**: Converter-based generator, Inertia-free stand-alone microgrid, Power balancing, Pure renewable energies based system, Superconducting flywheel energy storage system

## 1. Introduction

The electrical power systems are facing huge challenge because they are an important part of sustaining life for human beings. As part of the effort, many renewable energies based distributed generations (DGs) have been studied and substantiated by people in academia and industry. The renewable energies based DGs increase the number of DC-to-AC converters by generating DC power. For example, a photovoltaic (PV) initially generates DC power based on its intrinsic structure, and power from a wind-turbine (WT) is rectified before being supplied to the electrical grid due to the synchronization issue. Also, many energy storage devices, such as battery energy storage system (BESS), superconducting magnetic energy storage (SMES), and flywheel energy storage system (FESS), require the DC-to-AC converter to be connected to the electrical grid.

Several countries have made plans to build up stand-alone microgrid based on 100% renewable energies for carbon-free self-powered islands. For example, the president of Korea spoke about a "carbon-free Jeju by 2030" at COP21. A stand-alone microgrid with 100% renewable energies becomes inertia-free. This is because the microgrid is powered by the only converters, and inertia cannot be provided by the rotating masses of conventional generators. The zero inertia constant, $H$ causes large frequency deviation even if there is small error between input and output powers, $P_{\text{in}}$ and $P_{\text{out}}$ according to (1). Therefore, an inertia-free stand-alone (IFSA) microgrid becomes unstable unless the frequency, $\omega$ is properly controlled by the DC-to-AC converters.

$$\frac{d\omega}{dt} = \frac{\omega_0}{2H}\left(P_{\text{in}} - P_{\text{out}}\right) \tag{1}$$

To provide robust frequency and voltage, a diesel generator or large BESS is used for real stand-alone microgrids in Korea [1-3]. This balances the power between the generator and load, so that the state-of-charge (SOC) can indicate the power balance condition. In practice, however, the SOC is not directly measured but estimated [4, 5], and its estimation error is accumulated with the course of time. Although the FESS can provide a rotational speed without an accumulated error, it has considerable loss. In this paper, a superconducting FESS (SFESS) is used in consideration of the problems above.

This paper is organized as follows: Section 2 explains the IFSA microgrid with an SFESS. Next, several case studies are carried out in Section 3 using a microgrid model based on practical data. Finally, conclusions are given in Section 4.

† Corresponding Author: Korea Electrotechnology Research Institute (KERI), Korea. (slee82@keri.re.kr)
* School of Electrical and Electronic Engineering, Yonsei University, Korea. ({bsunho, igo87, jungpark}@yonsei.ac.kr)
Received: November 1, 2016; Accepted: May 24, 2017

## 2. IFSA Microgrid with SFESS

### 2.1 IFSA microgrid

The IFSA microgrid is powered by the only converter-based- generators (CBGs) as shown in Fig. 1. In the microgrid, most of the energy comes from renewable energies based generators such as PV and WT. The fuel cell (FC) contributes only a small part of energy generation by compensating for deficient power when the renewable energy is insufficient. In spite of the FC's small contribution to the total energy, it is important to mitigate the intermittent generation of renewable energies. Meanwhile, the SFESS contributes to an instant power balance.

In general, a grid connected DC-to-AC converter operates in constant power control mode as shown in Fig. 2 [6-8]. Parameters, $P$, $Q$, $P_{ref}$, and $Q_{ref}$ are the real power, reactive power, and their references, respectively. Based on $P$ and $Q$ errors, the $d$-$q$ axes current references, $I_{d,ref}$ and $I_{q,ref}$ are first determined. This is because $P$ and $Q$ are theoretically calculated by (2) and (3), respectively [9, 10].

$$P=V_d \cdot I_d + V_q \cdot I_q \tag{2}$$
$$Q=V_d \cdot I_q - V_q \cdot I_d \tag{3}$$

where $V_d$ is given by the grid and $V_q$ is almost zero. Next, $I_d$ and $I_q$ errors generate the converter control signals, $V_{sd}$ and $V_{sq}$ through a decoupling calculation of the $d$-$q$ axes. For decoupling, $X_f$ is set with a terminal impedance including filter.

The constant power controller requires the grid voltage as input, so that at least one converter must operate in

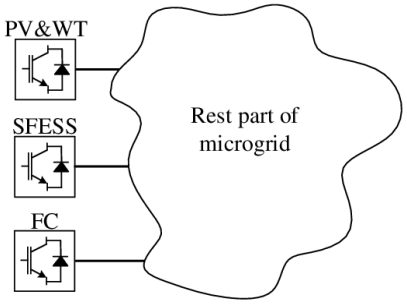


**Fig. 1.** Conceptual illustration of IFSA microgrid

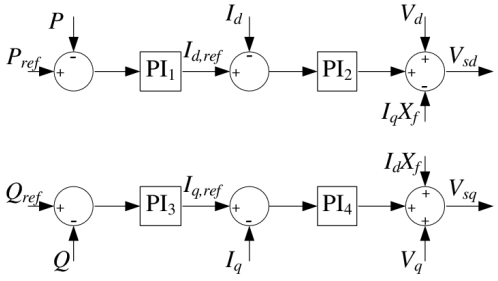


**Fig. 2.** Constant power control for grid-connected DC-to-AC converter

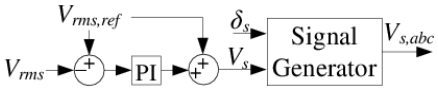


**Fig. 3.** Constant voltage control with fixed frequency

constant voltage control mode as shown in Fig. 3. In general, the reference root-mean-square (RMS) grid voltage, $V_{rms,ref}$ is set to 1 pu, and the RMS grid voltage error, $V_{rms,ref}$ - $V_{rms}$ determines the magnitude of terminal voltage, $V_s$. Phase angle, $\delta_s$ is set to zero when only one converter operates in constant voltage control mode. The load flow must be considered to determine phase angles when multiple converters operate in the voltage control mode. After $V_s$ and $\delta_s$ are determined, pure sinusoidal voltage references are generated by

$$\begin{aligned} V_{s,a} &= V_s \cos(120\pi \cdot t + \delta_s) \\ V_{s,b} &= V_s \cos(120\pi \cdot t + \delta_s - 2\pi/3) \\ V_{s,c} &= V_s \cos(120\pi \cdot t + \delta_s + 2\pi/3) \end{aligned} \tag{4}$$

Consequently, the converter operates as a slack generator, which balances the power between the generators and loads.

### 2.2 Power Balance using SFESS

The kinetic energy of rotating mass, $E_K$ is formulated as

$$E_K = \frac{1}{2} H \omega^2 \tag{5}$$

where $H$ and $\omega$ are the inertia constant and angular speed in per unit, respectively. Then, mechanical torque, $T_m$ is formulated as

$$T_m = H \frac{d\omega}{dt} \tag{6}$$

In mathematical terms, $T_m$, $H$, and $\omega$, can be considered as current, capacitance, and voltage, respectively. Therefore, the SFESS can be modeled with electrical components as shown in Fig. 4. Current sources carry out a power conversion between the DC-link and rotor. Parameters, $C$

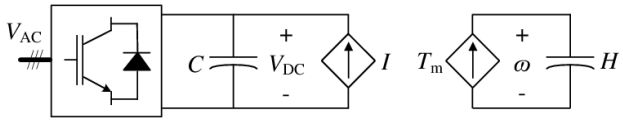


**Fig. 4.** Electrical model of SFESS

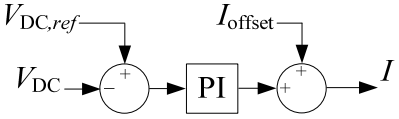


**Fig. 5.** DC-link voltage control

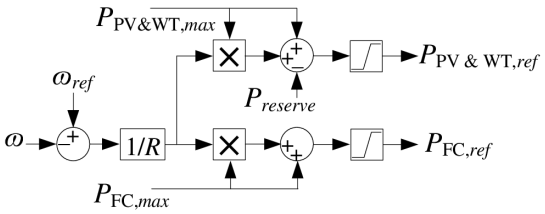


**Fig. 6.** Power balancing control based on SFESS frequency

and $I$ are the capacitance and current in the DC-link, respectively [11].

The AC terminal voltage, $V_{AC}$ is determined by $V_{s,abc}$ and the DC-link voltage, $V_{DC}$. Therefore, to supply robust voltage to the grid, $V_{DC}$ must be regulated. For its regulation, the DC-link voltage controller in Fig. 5 is applied to the SFESS model.

In practice, there is conversion loss between mechanical and electrical powers. It is carried out using conversion efficiency, $\alpha$, which is smaller or larger than 1 according to whether the SFESS is being charged or discharged. $T_m$ is determined by the mathematical relationship of (7), (8).

$$T_m = \frac{P_m}{\omega} = \frac{-\alpha P_e}{\omega} \tag{7}$$

$$P_e = P_L - P_{gen} = I \cdot V_{DC} \tag{8}$$

where $P_L$ and $P_{gen}$ are the load consumption and power generation, respectively. Therefore, the power balance condition can be indicated by the angular speed of the SFESS. The CBGs in the IFSA microgrid can properly control their real powers based on the angular speed of the SFESS instead of the microgrid frequency as shown in Fig. 6 where droop ratio, $R$ is determined in consideration of SFESS size. In the renewable generation control part, $P_{PV\&WT,\ max}$, $P_{reserve}$, and $P_{PV\&WT,\ ref}$ are maximum capability based on renewable energies conditions, power reserves for instant power balancing, and power reference, respectively. In the fuel cell generation control part, $P_{FC,\ max}$ and $P_{FC,\ ref}$ are the maximum power capacity and power reference, respectively.

## 3. Case Studies

To verify the proposed control, a microgrid is implemented with four loads (each 9 MW), 15 SFESSs (each 240 kW), one PV&WT (27 MW), and one FC (18 MW) as shown in Fig. 7. The PV&WT operates as a main generator group, and the FC operates to compensate for deficient power. In other words, the FC stops when PV&WT can generate sufficient power to cover the entire load. Also, PV&WT are operated with reserve power rather than with MPPT. Because the system stability is more important, power loss occurs in normal state.

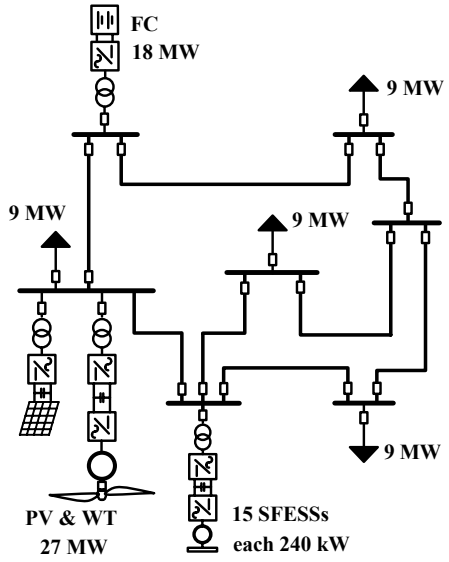


**Fig. 7.** IFSA microgrid with SFESS

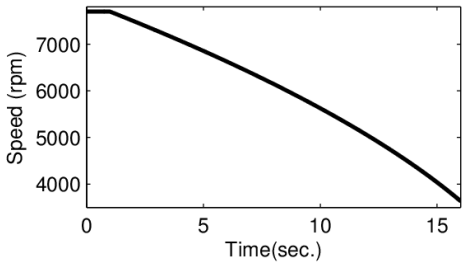


**Fig. 8.** Case A: angular speed of SFESS with rated output of 240 kW

### 3.1 Characteristics of SFESS

The main parameters of the SFESS model are selected based on a commercial FESS, which can store rotational kinetic energy up to 7,700 rpm and supply 240 kW up to 15 s. This is accomplished using a rotating solid cylinder with evenly distributed 600 lbs. of mass and a 25.5 in. diameter. Then, its inertia and minimum angular speed are derived as 14.276 kg·m2 and 3647 rpm, respectively. As shown in Fig. 8, the angular speed of the SFESS model is changed from 7,700 rpm to 3,647 rpm with a rated output of 240 kW for 15 s (1 to 16 s). That is, the model properly reflects the real SFESS.

### 3.2 Load changes without angular speed based control

In case B, the PV&WT and FC initially generate 26 MW and 8 MW, respectively. The initial load consumption is 34 MW, and 8.5 MW is decreased at 1 s. After the load reduction, the terminal voltages, powers, and frequency are regulated by the slack converter, which absorbs the surplus power, as shown in Fig. 9. However, the DC-link voltage

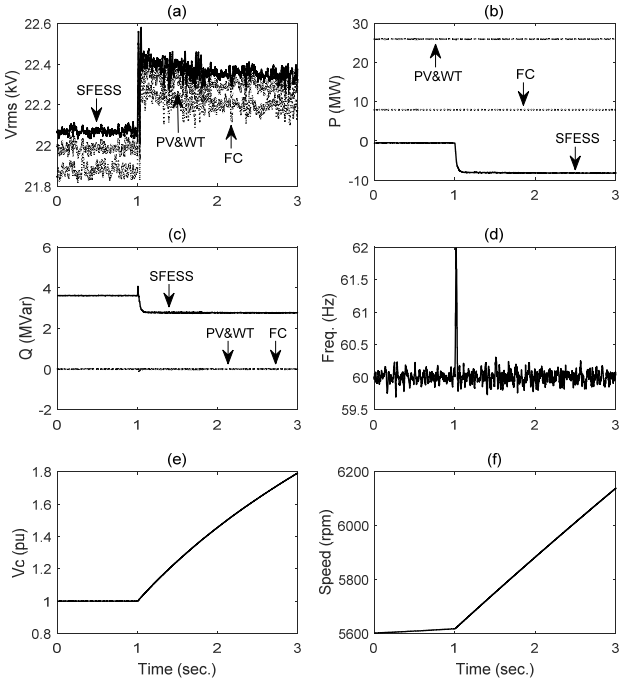


**Fig. 9.** Case B: responses for 8.5 MW load decrease at 1 s without $\omega$ based control: (a)-(c) responses of SFESS (solid line), PV&WT (dash-dotted line), and FC (dotted line) (d) microgrid frequency, (e) DC-link capacitor voltage of SFESS, and (f) angular speed of rotor in SFESS

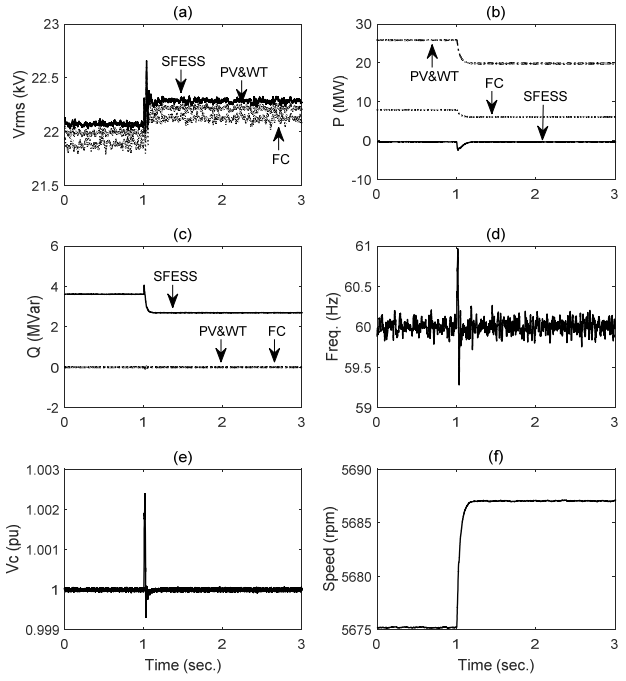


**Fig. 11.** Case D: responses for 8.5 MW load decrease at 1 s with $\omega$ based control: (a)-(c) responses of SFESS (solid line), PV&WT (dash-dotted line), and FC (dotted line) (d) microgrid frequency, (e) DC-link capacitor voltage of SFESS, and (f) angular speed of rotor in SFESS

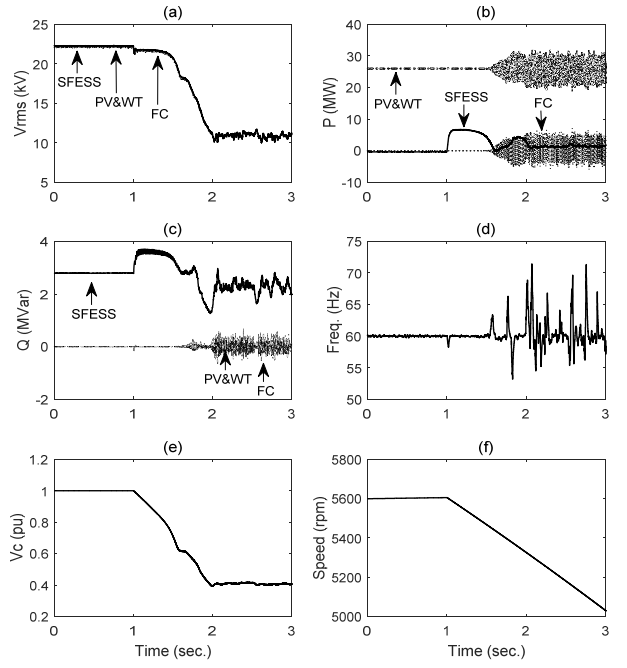


**Fig. 10.** Case C: responses for 8.5 MW load increase at 1 s without $\omega$ based control: (a)-(c) responses of SFESS (solid line), PV&WT (dash-dotted line), and FC (dotted line) (d) microgrid frequency, (e) DC-link capacitor voltage of SFESS, and (f) angular speed of rotor in SFESS

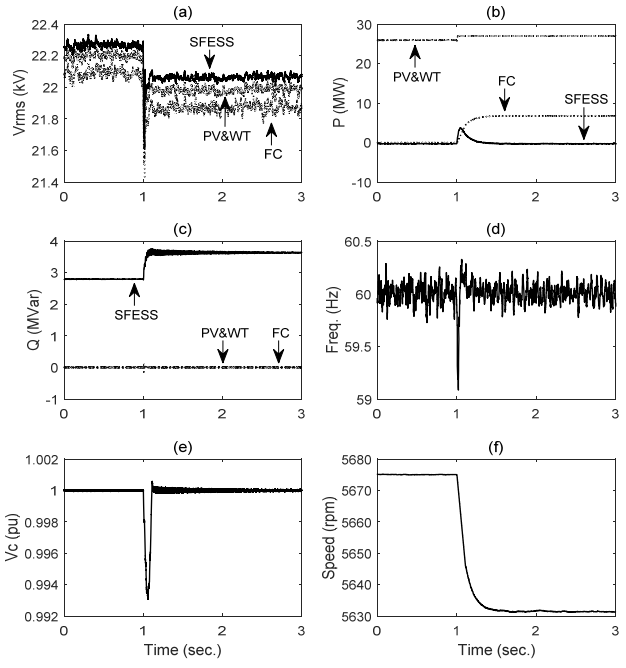


**Fig. 12.** Case E: responses for 8.5 MW load increase at 1 s with $\omega$ based control: (a)-(c) responses of SFESS (solid line), PV&WT (dash-dotted line), and FC (dotted line) (d) microgrid frequency, (e) DC-link capacitor voltage of SFESS, and (f) angular speed of rotor in SFESS

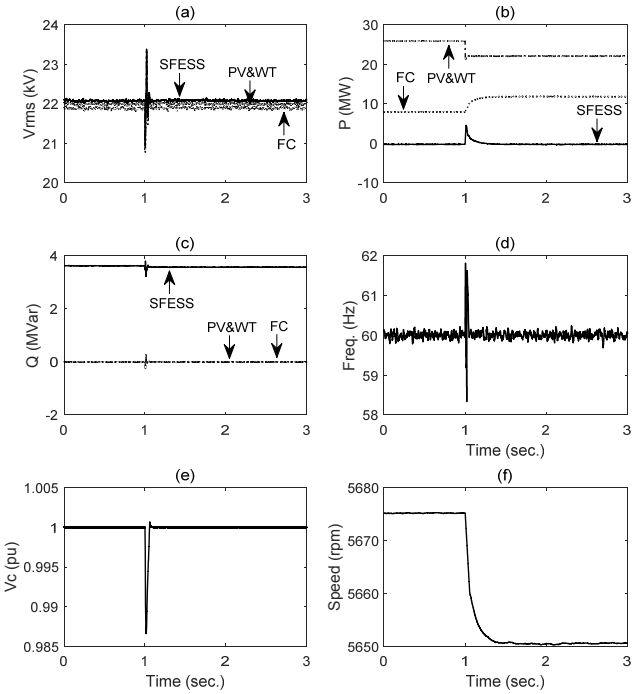


**Fig. 13.** Case F: responses for 5 MW renewable generation reduction at 1 s with $\omega$ based control: (a)-(c) responses of SFESS (solid line), PV&WT (dash-dotted line), and FC (dotted line) (d) microgrid frequency, (e) DC-link capacitor voltage of SFESS, and (f) angular speed of rotor in SFESS

increases because the SFESS can absorb at most 3.6 MW (i.e., 15 × 240 kW). The angular speed of the SFESS also increases due to the absorbed power.

In case C, the PV&WT and FC initially generate 26 MW and 0 MW, respectively. The initial load consumption is 26 MW, and 8.5 MW is increased at 1 s. After the load increase, the terminal voltages, powers, and frequency are regulated by the slack converter, which supplies the deficient power, as shown in Fig. 10. However, the DC-link voltage decreases because the SFESS can supply at most 3.6 MW. The angular speed of the SFESS also decreases due to the released power.

The case B and C in load change situations without angular speed based control show that the system becomes unstable and the DC-link voltage cannot be controlled.

### 3.3 Load changes with angular speed based control

In case D and E, Initial conditions and event are set to be the same in cases B and C except for the angular speed based control. The terminal voltages, powers, and frequency are regulated as shown in Figs. 11 and 12. In contrast to cases B and C, the DC-link voltage and the angular speed are regulated. This is because the PV&WT and FC respond to the angular speed of the SFESSs, and relieve the burden of the SFESSs.

### 3.4 Reduced PV&WT with angular speed based control

In case F, the initial conditions are the same for case B and control is the same for case D. To show the effects of intermittent renewable energies, the PV&WT CBG reduces 5 MW of real power at 1 s. The terminal voltages, powers, and frequency are regulated as shown in Fig. 13. In the same manner as case D, the DC-link voltage and the angular speed are regulated. According to the reduced angular speed of the SFESS, the FC increases its output power, so that it compensates the deficient 5 MW.

## 4. Conclusion

The IFSA microgrid is implemented with the only converters, so that it has no inertia. In other words, the system frequency in the IFSA microgrid is determined by the converter controls without regard to power balance. To stabilize the IFSA microgrid, therefore, at least one DC-to-AC converter must provide robust system frequency and voltage, and its power source must be controllable. The SFESS can inherently play that role using its stored kinetic energy for a short time. To consistently carry out that function, the SFESS provides an index of power balance to the IFSA microgrid based on the angular speed of its rotor. The index makes the CBGs properly share the mismatched power, so that the angular speed maintains its appropriate level. The proposed method successfully stabilizes the IFSA microgrid even if the power mismatch is much larger than the size of the SFESS.

Using the proposed technology, microgrids can be operated without diesel generators or grid-connections. Therefore, it is expected that this study will encourage growth in pure renewable energies based microgrids.

## Acknowledgement

This work was supported in part by the National Research Foundation of Korea (NRF) grant funded by the Korea government (MEST) (no. 2016R1E1A1A02920095) and in part by the Power Generation & Electricity Delivery Core Technology Program of the Korea Institute of Energy Technology Evaluation and Planning (KETEP) granted financial resource from the Ministry of Trade, Industry & Energy, Republic of Korea (no. 20141020402340).

## References

[1] S. H. Kim, I. Y. Chung, and W. K. Chae, "Voltage and Frequency Control Method Using Battery Energy Storage System for a Stand-alone Microgrid,"

*Trans. Korean Inst. Electr. Eng.*, vol. 64, no. 8, pp. 1168~1179, Aug. 2015.
[2] W. H. Hwang, S. K. Kim, J. H. Lee, W. K. Chae, J. H. Lee, H. J. Lee, and J. E. Kim, "Autonomous Micro-grid Design for Supplying Electricity in Carbon-Free Island," *J. Electr. Eng. Technol.* vol. 9, no. 3, pp. 1112-1118, Sept. 2014.
[3] W. K. Chae, H. J. Lee, J. N. Won, J. S. Park, and J. E. Kim, "Design and Field Tests of an Inverted Based Remote MicroGrid on a Korean Island," *Energies*, pp. 8193-8201, Aug. 2015.
[4] C. Zhang, L. Y. Wang, X. Li, W. Chen, G. G. Yin, and J. Jiang, "Robust and Adaptive Estimation of State of Charge for Lithium-Ion Batteries," *IEEE Trans. on Industrial Electronics*, vol. 62, no. 8, pp. 4948-4957, Aug. 2015.
[5] Y. Hu and Y. Y. Wang, "Two Time-Scaled Battery Model Identification With Application to Battery Stage Estimation," *IEEE. Trans. on Control Systems Technology*, vol. 23, no. 3, pp. 1180-1188, May 2015.
[6] X. Sun, Y, Tian, and Z. Chen, "Adaptive decoupled power control method for inverter connected DG," *IET Renewable Power Generation*, vol. 8, no. 2, pp. 171-182, Mar. 2014.
[7] H. Nian, Y. Shen, H. Yang, and Y. Quan, "Flexible Grid Connection Technique of Voltage-Source Inverter Under Unbalanced Grid Conditions Based on Direct Power Control," *IEEE Trans. on Industry Applications*, vol. 51, no. 5, pp. 4041-4050, Sept. 2015.
[8] P. Cheng and H. Nian, "Direct power control of voltage source inverter in a virtual synchronous reference frame during frequency variation and network unbalance," *IET Power Electronics*, vol. 9, no. 3, pp. 502-511, Mar. 2016.
[9] Taylor & Francis Group, Boca Raton, *Power System Stability and Control*, 2nd ed., FL, 2007, pp. 113-114.
[10] P. Cheng and H. Nian, "Direct power control of voltage source inverter in a virtual synchronous reference frame during frequency variation and network unbalance," *IET Power Electronics*, vol. 9, no. 3, pp. 502-511, Mar. 2016.
[11] R. P. Alzola, D. C. Gaona, and M. Ordonez, "Control of Flywheel Energy Storage Systems as Virtual Synchronous Machines for Microgrids," *in proc. of IEEE 16th Workshop on Control and Modeling for Power Electronics*, pp. 1-7, July 2015.

**SunHo Bae** received the B.S. degree from the Department of Mechanical and Control Engineering, Handong University, Pohang, Korea, in 2010. He is currently working toward the Ph.D. degree in a combined M.S. and Ph.D. program at Yonsei University, Seoul, Korea. His research interests include power control of electric vehicle, hardware implementation of grid-connected inverter with photovoltaic and energy storage devices, and energy management system for optimization of hybrid energy storage systems.

**DongHee Choi Lee** received the B.S. and Ph.D. degrees of electrical engineering from the School of Electrical and Electronic Engineering, Yonsei University, Seoul, Korea, in 2012 and 2017, respectively. He is currently a Post-doctoral Research Associate in the School of Electrical and Electronic Engineering, Yonsei University, Seoul, Korea. His research interests are power system operation and control, renewable energies based distributed generation, operation of stand-alone microgrid of islanded area, and optimal coordination of distributed generation systems.

**Jung-Wook Park** was born in Seoul, Korea. He received the B.S. degree (summa cum laude) from the Department of Electrical Engineering, Yonsei University, Seoul, Korea, in 1999, and the M.S.E.C.E. and Ph.D. degrees from the School of Electrical and Computer Engineering, Georgia Institute of Technology, Atlanta, USA in 2000 and 2003, respectively. He was a Post-doctoral Research Associate in the Department of Electrical and Computer Engineering, University of Wisconsin, Madison, USA during 2003-2004, and a Senior Research Engineer with LG Electronics Inc., Korea during 2004-2005. He is currently an Associate Professor in the School of Electrical and Electronic Engineering, Yonsei University, Seoul, Korea. He is now leading the National Leading Research Laboratory (NLRL) designated by Korea government to the subject of integrated optimal operation for smart grid. His current research interests are in power system dynamics, renewable energies based distributed generations, power control of electric vehicle, and optimization control algorithms. Prof. Park was the recipient of the Young Scientist Presidential Award in 2013 from the Korean Academy of Science and Technology (KAST), Korea.

**Soo Hyoung Lee** received the B.S. and Ph.D. degrees of electrical engineering from the School of Electrical and Electronic Engineering, Yonsei University, Seoul, Korea, in 2008 and 2012, respectively. He was a Post-doctoral Research Associate in the School of

Electrical and Computer Engineering, Georgia Institute of Technology, Atlanta, GA, USA during 2012-2014. He is currently a Senior Researcher in the Advanced Power Grid Research Division, Korea Electrotechnology Research Institute (KERI). He was the recipient of the Gold Prize Paper Award from the TMS (Telecommunication, Multimedia, and SOC) Institute of Technology and Second Prize Paper Award from the Yonsei Electric Power Research Center. His research interests are converter based microgrid, optimal coordination of distributed generation systems, converter control for distributed generation systems, and implementation of multi-level converters.